



Published in final edited form as:

Prog Cardiovasc Dis. 2017 ; 60(3): 361–369. doi:10.1016/j.pcad.2017.10.007.

Mitral Valve Prolapse: Multimodality Imaging and Genetic Insights

Purvi Parwani¹, Jean-Francois Avierinos², Robert A. Levine³, and Francesca Nesta Delling¹

¹Department of Medicine, Division of Cardiology, University of California San Francisco, San Francisco, CA

²Department of Cardiology, APHM, La Timone Hospital, Marseille, France

³Cardiac Ultrasound Laboratory, Department of Medicine, Massachusetts General Hospital, Harvard Medical School, Boston, MA

Abstract

Mitral valve prolapse (MVP) is a common heritable valvulopathy affecting approximately 2.4% of the population. It is the most important cause of primary mitral regurgitation (MR) requiring surgery. MVP is characterized by fibromyxomatous changes and displacement of one or both mitral leaflets into the left atrium. Echocardiography represents the primary diagnostic modality for assessment of MVP. Accurate quantitation of ventricular volumes and function for surgical planning in asymptomatic severe MR can be provided with both echocardiography and cardiac magnetic resonance. In addition, assessment of myocardial fibrosis using late gadolinium enhancement and T1 mapping allows better understanding of the impact of MVP on the myocardium. Imaging in MVP is important not only for diagnostic and prognostic purposes, but is also essential for detailed phenotyping in genetic studies. Genotype-phenotype studies in MVP pedigrees have allowed the identification of milder, non-diagnostic MVP morphologies by echocardiography. Such morphologies represent early expression of MVP in gene carriers. This review focuses on multimodality imaging and the phenotypic spectrum of MVP. Moreover, the review details the recent genetic discoveries that have increased our understanding of the pathophysiology of MVP, with clues to mechanisms and therapy.

Keywords

Cardiac Magnetic Resonance; Echocardiography; Genetics; Mitral Valve Prolapse; Mitral Regurgitation

Corresponding Author: Francesca Nesta Delling, MD, MPH, University of California San Francisco, Smith Cardiovascular Research Building MC3120, 555 Mission Bay Blvd South, Room S352C, San Francisco, CA 94158, Phone: 415-514-0992/Fax: 415-502-7949, Francesca.Delling@ucsf.edu.

Disclosures: None

Conflict of interest: None.

Publisher's Disclaimer: This is a PDF file of an unedited manuscript that has been accepted for publication. As a service to our customers we are providing this early version of the manuscript. The manuscript will undergo copyediting, typesetting, and review of the resulting proof before it is published in its final citable form. Please note that during the production process errors may be discovered which could affect the content, and all legal disclaimers that apply to the journal pertain.

INTRODUCTION

Mitral valve (MV) prolapse (MVP) is a common heritable valvulopathy affecting over 7 million individuals in the United States and over 170 million worldwide.(1; 2) It is the most important cause of primary mitral regurgitation (MR) requiring surgery.(3; 4) MVP is characterized by fibromyxomatous changes, defined by expansion of the middle spongiosa layer of the valve (due to an accumulation of proteoglycans), structural alterations of collagen in all components of the leaflet, and by structurally abnormal chordae.(5; 6) Dysregulation of the extra-cellular matrix (ECM) components plays a key role in mediating these changes and is essential to understand the genetic pathways leading to MVP.

MVP is defined by echocardiography as displacement greater than 2 mm of one or both leaflets beyond the annular high points at end-systole (Figure 1A–B).(7–9) Leaflet displacement is responsible for malcoaptation and consequent MR. Although most individuals with MVP in the general population have mild or no MR,(10) severe MR can occur in almost 10% of subjects with MVP(1) and more in the clinical population.(11) MVP can also lead to arrhythmias, heart failure, infective endocarditis, congestive heart failure and sudden cardiac death.(3; 5; 6) In light of the adverse prognosis in a subset of MVP patients, imaging becomes an essential tool to better understand mechanisms and identify those at higher risk. Moreover, recent genetic discoveries may provide additional clues to MVP mechanisms, with the potential of developing medical therapies.

The main objectives of this review are to: 1) Describe the use of different imaging modalities in the diagnosis and prognosis of MVP. 2) Summarize the current knowledge on the genetics of MVP based on its current classification. 3) Describe how echocardiography has helped with discovery of early or non-diagnostic MVP morphologies through detailed genotype-phenotype correlations in MVP pedigrees.

CLASSIFICATION OF MVP

MVP can be classified as non-syndromic or syndromic. Non-syndromic MVP can be familial or sporadic. Syndromic MVP occurs in association with connective tissue disorders such as Marfan syndrome, Loeys-Dietz Syndrome, Ehler-Danlos syndrome, osteogenesis imperfecta, Pseudoxanthoma Elasticum and aneurysms of osteoarthritis syndrome.(12–16)

Based on intraoperative findings and histological phenotype, degenerative MV disease has also been classified into two distinct entities in the surgical literature: Barlow's disease (BD) and fibro-elastic deficiency (FED).(17) BD (18; 19) is characterized by excessive leaflet tissue, diffusely thickened and distended leaflets, enlarged mitral annulus and multi-scallop prolapse. In patients with FED, there is typically focal thickening and prolapse of the middle segment of the posterior leaflet with thin chordae that frequently rupture causing flail leaflet and acute MR.

MULTIMODALITY IMAGING OF MVP

Mitral valve anatomy

A description of the anatomy of the MV is essential to fully understand the role of multimodality imaging in MVP. Anatomically, the anterior and posterior mitral leaflets are both divided into 3 scallops based on the Carpentier's nomenclature:(20) the anterior leaflet scallops are described as lateral (A1), medial (A3) and middle (A2); the posterior leaflet segments are known as lateral (P1), medial (P3) and middle (P2) (Figure 1C).

Echocardiography

In the early days of two-dimensional (2D) echocardiography, the diagnosis of MVP occurred with prevalence ranging from 5 to 15%, and even as high as 35%.(21; 22) In part, this over-diagnosis was due to the erroneous assumption that the MV annulus was planar; thus, displacement of the leaflets beyond the mitral annulus was deemed pathological in any echocardiographic view (including the 4-chamber view). Using three-dimensional (3D) echo imaging, it was later established that the mitral annulus was not planar, but saddle-shaped, with hinge points being best appreciated in the anterior-posterior axis (i.e. in the long-axis view).(7–9) Echocardiographic MVP has since been defined as single or bi-leaflet prolapse of greater than 2 mm beyond the long-axis annular plane (Figure 1A).(7–9) These revised diagnostic criteria were used in the Framingham Heart Study (FHS) to redefine the true prevalence of MVP. Freed et al. analyzed 3491 participants and reported that 84 patients had echocardiographic MVP (2.4%).(4) While the FHS had a predominantly Caucasian population, in a Canadian study (SHARE) utilizing the same diagnostic criteria, the prevalence of MVP was found to be similar between three different ethnic groups: South Asian (2.7%), European (3.1%), and Chinese (2.2%).(23)

In experienced hands, transthoracic echocardiography (TTE) allows for accurate identification of prolapsing MV scallops in most patients. Importantly, TTE is used as primary tool for comprehensive assessment of MVP-related MR. TTE can adequately quantify MR by use of various methods including the vena contracta, the proximal isovelocity surface area (PISA), and determination of MR regurgitant volume and fraction through pulsed-wave Doppler measurements.(24–27) Finally, TTE allows quantification of left atrial (LA) and left ventricular (LV) dimensions and function, which are both affected by clinically significant MR. (11) Considering several planes of imaging, 2D transesophageal echocardiography (TEE) can also be used to identify prolapsing MV segments (Figure 1B). (20) 3D TEE has the additional advantage of simulating the surgeon's view of the MV, with the aortic valve at the 11 o'clock position (Figure 1C), and has become an essential tool in the intra-operative setting. Sensitivity of intraoperative 3D TEE for detection of prolapsing scallops is around 94%.(28–32)

As no validated criteria exist, controversy remains about the ability of echocardiography to differentiate FED from BD. However, a recent 3D TEE study assessing valvular mechanics in FED and BD (also known as diffuse myxomatous degeneration) suggests that compared to BD, which is characterized by profoundly abnormal mitral annular dynamics and increased annular size, FED has a relatively normal annulus and normal annular dynamics in

patients with a similar degree of MR. Prolapse in FED is established early and increases little in systole; valvular tissue areas are stable. On the other hand, valvular area and prolapse increase considerably throughout systole in BD.(33)

Finally, 3D echocardiography has increased our understanding of the so-called mitral annular disjunction (MAD). MAD was initially described as a separation between the LA wall at the level of MV junction and the LV free wall (Figure 1A).(34) Although prevalence of actual mitral annular disjunction versus an elongated posterior leaflet abutting the posterior LA wall remains controversial, Eriksson et al.(35) reported a prevalence of MAD of around 98% on 2D TEE in patients with severe MVP-related MR. Later, Carmo et al. described MAD on routine TTE and found that MAD prevalence was around 55% in patients with a myxomatous MV with varying severity of MR.(36) In a recent 3D TEE study, Lee et al. demonstrated that the disjunctive annulus in MVP is decoupled functionally from the LV, leading to paradoxical annular dynamics with systolic expansion and flattening and greater MR.(37)

Cardiac Magnetic Resonance(CMR) Imaging

In recent years, CMR has emerged as an important noninvasive modality to characterize MVP (Figure 1D), and to determine LV volumes and function accurately. It also helps to quantify MR by using phase contrast velocity mapping.(38) Han et al. first demonstrated that CMR can identify MVP by the same echocardiographic criteria of 2 mm displacement beyond the mitral annulus.(39) Anterior leaflet length, posterior leaflet displacement, posterior leaflet thickness, and the presence of flail were later shown to be the best CMR valvular determinants of MVP-related MR.(40) CMR also allows better understanding of the interactions between MVP and the myocardium through improved spatial resolution provided by 3D acquisition of images with delayed or late gadolinium enhancement (LGE). (38; 41; 42) Specifically, papillary muscle (PM) fibrosis was identified using LGE in patients with MVP with a history of ventricular arrhythmias and at least moderate MR (Figure 2A).(39) Basso et al. later demonstrated that arrhythmic MVP was associated with fibrosis not only at the level of the PMs but also within the infero-basal wall. This was established in a series of patients who either died suddenly or presented with complex ventricular arrhythmias.(43) Interestingly, none of these individuals had significant MR. Unlike ischemic heart disease or cardiomyopathy, even a small focal LGE burden was associated with sudden cardiac death in patients with MVP. Perazzolo Marra et al. in 2016 found that MAD and systolic curling of the posterior MV leaflet were present in sudden cardiac death cases with LGE in the LV infero-basal wall.(44)

Whereas LGE typically identifies focal fibrosis, myocardial tissue characterization using either native/pre-contrast or post-contrast T₁ mapping allows for accurate quantitative assessment of interstitial or diffuse fibrosis. Abnormal T₁ mapping has been demonstrated in asymptomatic patients with MVP and moderate-severe MR (Figure 2B).(45) Recently, diffuse interstitial derangement by CMR was linked to subclinical systolic LV dysfunction and ventricular arrhythmia in MVP-related MR, even in the absence of focal fibrosis.(46)

Computed Tomography (CT)

The role of CT in patients with MVP with limited acoustic windows has been previously described in the literature. CT offers better spatial resolution and simultaneously evaluation of coronary artery disease. Cardiac CT is around 84.6% sensitive and 100% specific for assessment of MV abnormalities.(47) Radiation exposure, poor temporal resolution and limited ability to examine each leaflet are some of the important limitations of cardiac CT for evaluation of MVP.

GENETICS OF MVP

Non-Syndromic MVP

Knowledge of MVP inheritance was initially based on the use of physical examination or M-mode echocardiography in MVP pedigrees. Hancock and Cohn in 1966 found systolic clicks and murmurs in different generations of MVP families and suggested a familial genetic basis.(48)

In later echocardiographic and auscultatory studies, 50% of first-degree relatives were found to be affected by MVP.(49) In 1975, Weiss suggested an autosomal dominant pattern of inheritance after noticing one parent involvement in each pair examined.(50) The extent of familial clustering of MVP among unselected individuals in the community based on current, more specific 2D echocardiographic criteria was recently investigated in the FHS community,(51) where parental MVP was associated with a higher prevalence of MVP in the offspring compared to non-parental MVP (adjusted odds ratio [OR], 4.51, 95% confidence interval [CI], 2.13–9.54).(51)

Discovery of the first genetic loci for autosomal dominant, non-syndromic MVP occurred in the late 1990s only after better understanding of the 3D shape of the MV and improved specificity of MVP diagnosis.(7–9) The first locus was mapped to chromosome 16p11.2–p12.1 (*MMVP1*) by Disse et al. in 1999 in a multigenerational pedigree.(52) Linkage analysis yielded a maximal multipoint likelihood of the odds (LOD) score of 5.6. This was confirmed by haplotype analysis demonstrating that a chromosomal region of about 5 centimorgans (cM) (or 5 million DNA base pairs) contained the locus. To date, a specific gene mutation causing MVP in this pedigree has not been identified. A second locus was mapped to 11p15.4 (*MMVP2*) by Fred et al. in 2003.(53) Multipoint parametric analysis gave a maximum LOD score of 3.12. Haplotype analysis across this locus defined a 4.3 cm region. A third chromosomal locus for autosomal dominant MVP was mapped to chromosome 13q31.3–q32 in 2005 with a multipoint LOD score of 3.17 (*MMVP3*).(54) The risk haplotype involved an 8 million DNA pair dense chromosomal segment. The discovery of *MMVP3* not only confirmed the genetic heterogeneity of MVP, but also provided important clinical lessons. Specifically, phenotyping of the *MMVP3* pedigree revealed “non-diagnostic” MVP morphologies previously considered to be normal variants but now for the first time recognized as having the same genetic substrate as fully affected family members. (54)

X-linked myxomatous valvular dystrophy is a rare myxoid heart disease first described in 1998.(55) It is characterized by similar histopathological changes when compared to the

more common autosomal dominant MVP. However, it is characterized by multi-valvular rather than isolated MV myxomatous degeneration. The first investigation was performed in a large family of 4 generations (92 individuals) with full penetrance of MVP in the men of the family. The locus was mapped to a sex chromosome, Xq28 with LOD score of 6.57. Using a familial and genealogical survey, Kyndt et al. further refined the X-linked myxomatous valvular dystrophy locus to a 2.5-Mb region. Standard positional cloning identified a P637Q mutation in the filamin A (*FLNA*) gene in all affected members.(56) Two other missense mutations (G288R and V711D) and a 1944-bp genomic deletion coding for exons 16 to 19 in the *FLNA* gene were identified in 3 additional, smaller, unrelated families affected by valvular dystrophy, thus corroborating the role of *FLNA* as a cause of X-linked myxomatous valvular dystrophy and allowing discovery of the first MVP gene. Among carriers of the *FLNA* mutation, the penetrance of the disease was complete in men and incomplete in women. Female carriers could be mildly affected, and the severity of the disease was highly variable among mutation carriers.

Filamins (A, B and C) were initially described as non-muscle actin binding proteins.(57) Filamin A and B are ubiquitously expressed in the tissue while filamin C is expressed primarily in cardiac and skeletal muscle. Filamins interact with 30 different proteins including both actin and membrane protein and play a major role in building the cytoskeleton. Filamin A is responsible for regulation of several cellular signaling pathway by interacting with critical signaling molecules like transforming growth factor-beta receptor activated smads and the dopamine receptor.(58) Work by Sauls et al. demonstrated that filamin-A-deficient mice exhibit abnormally enlarged mitral valves during fetal life, which progresses to a myxomatous phenotype by 2 months of age. The authors also showed that the inception of valve disease in such functional model was related to lack of organization of the ECM.(59)

Following discovery of the *FLNA* gene for the rare X-linked myxomatous valvular dystrophy, the first autosomal dominant MVP gene was identified in the *MMVP2* (or chromosome 11) family after performing capture sequencing of the *MMVP2* locus in four affected individuals. Specifically, a missense mutation in the *DCHS1* gene, the human homologue of the *Drosophila* cell polarity gene *dachsous* was found to segregate in the original *MMVP2* family. Further genetic studies identified two additional families in which a second deleterious *DCHS1* mutation segregated with MVP. A knockdown *DCHS1* mouse model revealed prolapse of thickened and myxomatous MV leaflets, which could be traced back to developmental errors in valve morphogenesis.(60)

After the initial family studies, the first meta-analysis of two independent French genome-wide association studies was performed in 1,412 MVP cases and 2,439 controls for ~4.8 million genotyped or imputed common (minor allele frequency] > 0.1) single nucleotide polymorphisms.(61) Six loci showed genome-wide significant association with MVP. These loci were replicated in 1,422 cases and 6,779 controls. Functional models highlighted the role of *LMCD1* (LIM and cysteine-rich domains 1), which encodes a transcription factor 6 and for which the knockdown zebrafish model resulted in atrioventricular valve regurgitation. A similar zebrafish phenotype was obtained with knockdown of *TNSI*, which encodes tensin 1, a focal adhesion protein involved in cytoskeleton organization. The authors

showed expression of tensin 1 during valve morphogenesis and described enlarged and myxomatous posterior mitral leaflets in knockdown *TNSI* mice.

Common denominator of all genetic discoveries detailed above is the valvular phenotype of myxomatous degeneration described in both humans and mice models. Although many questions remain unanswered with regards to MVP mechanisms, these findings have increased our understanding of the pathophysiology of the common autosomal dominant MVP, with the potential to develop novel medical therapies.

Syndromic MVP

Syndromic MVP associated with connective tissue disorders displays similar degenerative myxomatous changes to non-syndromic MVP.(62)

Marfan syndrome is caused by mutations in fibrillin-1 (*FBN-1*)(63) and less commonly in TGF- receptor-2 (*TGFBR2*).(64) MVP can be identified in both genetic subtypes of Marfan syndrome. FBN-1 is an important structural component of the ECM and regulates TGF-beta availability. TGF-beta is responsible for ECM remodeling and valvular interstitial cell differentiation. Therefore, deficiency of fibrillin-1 results in increased TGF-beta expression. In vivo, the phenotypic expression of FBN-1 deficient mice was reversed by neutralizing antibodies against TGF-beta.(65) In a similar FBN-1 deficient mouse model, treatment with angiotensin II receptor blockade (losartan) lead to decrease in aortic root dilatation and MVP.(66) Overall, these findings highlight the potential to develop pharmacological therapies able to limit MVP progression at an early stage.

MVP has also been observed in the Loeys-Dietz syndrome, a connective tissue disease resulting from heterozygous mutations in the *TGFBR1* gene or the *TGFBR2* gene that encode subunits of the TGF- β receptor.(15) Valve tissue in these individuals demonstrates evidence of increased TGF- β activity. Heterozygous mutations in *MADH3* have been demonstrated in the aneurysms-osteoarthritis syndrome, another connective tissue disorder associated with MVP. *MADH3* encodes *SMAD3*, which is a positive regulator of TGF- β , again pointing to the role of TGF- β overexpression in myxomatous MV disease.(16)

GENOTYPE-PHENOTYPE CORRELATIONS IN MVP

Phenotyping of pedigrees during initial MVP genetic studies revealed a spectrum of MVP expression that included borderline, or “non-diagnostic,” valve morphologies previously considered to be normal variants.(53; 54) In such family studies, the concept of “normalcy” of non-diagnostic morphologies was challenged, as borderline morphologies shared either the complete or a major portion of the at-risk haplotype with fully diagnostic MVP.(54) Two types of non-diagnostic MVP morphologies have been described in the familial setting,(54) and more recently in the FHS community (Figure 3):(67) “abnormal anterior coaptation” (AAC) (Figure 3A) and minimal systolic displacement (Figure 3B). The AAC phenotype shared two salient features with fully diagnostic posterior MVP (Figure 3C): an anteriorly displaced coaptation point, and posterior leaflet asymmetry. Thus, AAC can be considered “geometrically congruent” with posterior MVP. Individuals with minimal systolic displacement shared the posterior leaflet asymmetry with full-blown MVP, but their

coaptation point was posterior (as in normal individuals). It was later demonstrated that parental non-diagnostic morphologies in FHS are associated with a higher prevalence of MVP in the offspring. Moreover, after a median follow-up of one decade, 80% of FHS participants with AAC and 24% of individuals with minimal systolic displacement evolve into fully diagnostic MVP.(4) Overall, these findings underline the clinical significance of mild MVP expression in the community.

PROGNOSIS OF MVP

The prognosis of MVP has varied in the published literature. In the community-based FHS, MVP was described as a benign entity, with a low occurrence of adverse sequelae.(1) In prior studies,(3; 5) MVP was portrayed as a disease with frequent and serious complications, including stroke, atrial fibrillation, endocarditis, heart failure, and MR requiring surgery. These discrepancies may be due to selection biases inherent in evaluating symptomatic patients at referral tertiary care centers, compared to observations made on healthier asymptomatic volunteers in the FHS.(1; 3; 5). Subsequently, a study from the Mayo Clinic, characterized by a mixed spectrum of community-dwelling and referred patients, has underscored the clinical heterogeneity of MVP, including a widely varying prognostic spectrum.(11) Based on primary (depressed LV ejection fraction, moderate/severe MR) and secondary (age > 50 years, mild MR, LA enlargement, atrial fibrillation, and flail leaflet) risk factors, different groups of MVPs with varying prognosis were identified with regards to cardiovascular morbidity and mortality.(11)

The common denominator of the studies evaluating prognosis of MVP is the role of MR at the time of diagnosis in determining the risk for adverse events.(1; 3; 5; 68–70) In a study of 456 individuals diagnosed with asymptomatic MVP and followed longitudinally in the Olmsted County, severe MR was a powerful predictor of death from any cause, death from cardiac causes, and cardiac events.

Independently and beyond MR, MV leaflet thickness >5 mm on echocardiography has been associated with increased risk for sudden death, stroke, endocarditis, and MR in patients with classic prolapse in some series (3; 5; 71; 72). LV end-systolic diameter and ejection fraction have also been shown to be important prognostic determinants, as both are independent predictors of post-operative ejection fraction.(73) TTE-defined bileaflet MVP, often associated with MAD, has been associated with increased risk of sudden cardiac death.(74) Overall, TTE remains the main tool of prognostic assessment of MVP in clinical practice. As described above, CMR nicely complements echocardiography by demonstrating myocardial fibrosis, a risk factor for arrhythmic complications and indicator of early systolic dysfunction. (43–46) Finally, the genetic substrate of MVP may one day complete risk stratification.

CONCLUSIONS

Echocardiography represents the primary diagnostic modality for assessment of MVP, although CMR is becoming an essential complement to echocardiography for accurate assessment of LV volumes and function, MR quantification, and arrhythmic risk

stratification in MVP. Imaging in MVP is important not only for diagnostic and prognostic purposes, but also for detailed phenotyping in genetic studies. Whereas *FLNA* has been identified as causing a rare X-linked form of MVP, mutations in *DCSH1* have been recently associated with the more common form of autosomal dominant MVP. In addition, a number of loci have been discovered both in MVP pedigrees and through a genome wide association study. Detailed echocardiographic phenotyping has played a major role in the identification of MVP genes and has highlighted the clinical significance of borderline or “non-diagnostic” MVP in the general population.

List of Abbreviations

AAC	Abnormal Anterior Coaptation
BD	Barlow’s Disease
CMR	Cardiac Magnetic Resonance
CT	Computed Tomography
FED	Fibro-Elastic Deficiency
FHS	Framingham Heart Study
LA	Left Atrial
LV	Left Ventricular
LGE	Late Gadolinium Enhancement
LoD	Likelihood of the Odds
MAD	Mitral Annular Disjunction
MV	Mitral Valve
MVP	Mitral Valve Prolapse
MR	Mitral Regurgitation
PM	Papillary Muscle
TEE	Transesophageal Echocardiogram
TTE	Transthoracic Echocardiogram

References

1. Freed LA, Levy D, Levine RA, Larson MG, Evans JC, et al. Prevalence and clinical outcome of mitral-valve prolapse. *N Engl J Med*. 1999; 341:1–7. [PubMed: 10387935]
2. Delling FN, Vasan RS. Epidemiology and pathophysiology of mitral valve prolapse: new insights into disease progression, genetics, and molecular basis. *Circulation*. 2014; 129:2158–70. [PubMed: 24867995]
3. Zuppiroli A, Rinaldi M, Kramer-Fox R, Favilli S, Roman MJ, Devereux RB. Natural history of mitral valve prolapse. *Am J Cardiol*. 1995; 75:1028–32. [PubMed: 7747683]

4. Delling FN, Rong J, Larson MG, Lehman B, Fuller D, et al. Evolution of Mitral Valve Prolapse: Insights From the Framingham Heart Study. *Circulation*. 2016; 133:1688–95. [PubMed: 27006478]
5. Devereux RB, Kramer-Fox R, Shear MK, Kligfield P, Pini R, Savage DD. Diagnosis and classification of severity of mitral valve prolapse: methodologic, biologic, and prognostic considerations. *Am Heart J*. 1987; 113:1265–80. [PubMed: 3554945]
6. Luxereau P, Dorent R, De Gevigney G, Bruneval P, Chomette G, Delahaye G. Aetiology of surgically treated mitral regurgitation. *Eur Heart J*. 1991; 12(Suppl B):2–4.
7. Levine RA, Handschumacher MD, Sanfilippo AJ, Hagege AA, Harrigan P, et al. Three-dimensional echocardiographic reconstruction of the mitral valve, with implications for the diagnosis of mitral valve prolapse. *Circulation*. 1989; 80:589–98. [PubMed: 2766511]
8. Levine RA, Stathogiannis E, Newell JB, Harrigan P, Weyman AE. Reconsideration of echocardiographic standards for mitral valve prolapse: lack of association between leaflet displacement isolated to the apical four chamber view and independent echocardiographic evidence of abnormality. *J Am Coll Cardiol*. 1988; 11:1010–9. [PubMed: 3281989]
9. Levine RA, Triulzi MO, Harrigan P, Weyman AE. The relationship of mitral annular shape to the diagnosis of mitral valve prolapse. *Circulation*. 1987; 75:756–67. [PubMed: 3829339]
10. Freed LA, Benjamin EJ, Levy D, Larson MG, Evans JC, et al. Mitral valve prolapse in the general population: the benign nature of echocardiographic features in the Framingham Heart Study. *J Am Coll Cardiol*. 2002; 40:1298–304. [PubMed: 12383578]
11. Avierinos JF, Gersh BJ, Melton LJ 3rd, Bailey KR, Shub C, et al. Natural history of asymptomatic mitral valve prolapse in the community. *Circulation*. 2002; 106:1355–61. [PubMed: 12221052]
12. Hortop J, Tsiouras P, Hanley JA, Maron BJ, Shapiro JR. Cardiovascular involvement in osteogenesis imperfecta. *Circulation*. 1986; 73:54–61. [PubMed: 3940669]
13. Roman MJ, Devereux RB, Kramer-Fox R, Spitzer MC. Comparison of cardiovascular and skeletal features of primary mitral valve prolapse and Marfan syndrome. *Am J Cardiol*. 1989; 63:317–21. [PubMed: 2913733]
14. Rubegni P, Mondillo S, De Aloe G, Agricola E, Bardelli AM, Fimiani M. Mitral valve prolapse in healthy relatives of patients with familial Pseudoxanthoma elasticum. *Am J Cardiol*. 2000; 85:1268–71. [PubMed: 10802018]
15. Loeys BL, Schwarze U, Holm T, Callewaert BL, Thomas GH, et al. Aneurysm syndromes caused by mutations in the TGF-beta receptor. *N Engl J Med*. 2006; 355:788–98. [PubMed: 16928994]
16. van de Laar IM, Oldenburg RA, Pals G, Roos-Hesselink JW, de Graaf BM, et al. Mutations in SMAD3 cause a syndromic form of aortic aneurysms and dissections with early-onset osteoarthritis. *Nat Genet*. 2011; 43:121–6. [PubMed: 21217753]
17. Anyanwu AC, Adams DH. Etiologic classification of degenerative mitral valve disease: Barlow's disease and fibroelastic deficiency. *Semin Thorac Cardiovasc Surg*. 2007; 19:90–6. [PubMed: 17870001]
18. Carpentier A, Chauvaud S, Fabiani JN, Deloche A, Relland J, et al. Reconstructive surgery of mitral valve incompetence: ten-year appraisal. *J Thorac Cardiovasc Surg*. 1980; 79:338–48. [PubMed: 7354634]
19. Fornes P, Heudes D, Fuzellier JF, Tixier D, Bruneval P, Carpentier A. Correlation between clinical and histologic patterns of degenerative mitral valve insufficiency: a histomorphometric study of 130 excised segments. *Cardiovasc Pathol*. 1999; 8:81–92. [PubMed: 10724505]
20. Carpentier A. Cardiac valve surgery--the "French correction". *J Thorac Cardiovasc Surg*. 1983; 86:323–37. [PubMed: 6887954]
21. Savage DD, Devereux RB, Garrison RJ, Castelli WP, Anderson SJ, et al. Mitral valve prolapse in the general population. 2. Clinical features: the Framingham Study. *Am Heart J*. 1983; 106:577–81. [PubMed: 6881032]
22. Warth DC, King ME, Cohen JM, Tesoriero VL, Marcus E, Weyman AE. Prevalence of mitral valve prolapse in normal children. *J Am Coll Cardiol*. 1985; 5:1173–7. [PubMed: 3989128]
23. Theal M, Sleik K, Anand S, Yi Q, Yusuf S, Lonn E. Prevalence of mitral valve prolapse in ethnic groups. *Can J Cardiol*. 2004; 20:511–5. [PubMed: 15100753]

24. Vandervoort PM, Thoreau DH, Rivera JM, Levine RA, Weyman AE, Thomas JD. Automated flow rate calculations based on digital analysis of flow convergence proximal to regurgitant orifices. *J Am Coll Cardiol.* 1993; 22:535–41. [PubMed: 8335826]
25. Fehske W, Omran H, Manz M, Kohler J, Hagendorff A, Luderitz B. Color-coded Doppler imaging of the vena contracta as a basis for quantification of pure mitral regurgitation. *Am J Cardiol.* 1994; 73:268–74. [PubMed: 8296758]
26. Enriquez-Sarano M, Miller FA Jr, Hayes SN, Bailey KR, Tajik AJ, Seward JB. Effective mitral regurgitant orifice area: clinical use and pitfalls of the proximal isovelocity surface area method. *J Am Coll Cardiol.* 1995; 25:703–9. [PubMed: 7860917]
27. Sun JP, Yang XS, Qin JX, Greenberg NL, Zhou J, et al. Quantification of mitral regurgitation by automated cardiac output measurement: experimental and clinical validation. *J Am Coll Cardiol.* 1998; 32:1074–82. [PubMed: 9768735]
28. Salustri A, Becker AE, van Herwerden L, Vletter WB, Ten Cate FJ, Roelandt JR. Three-dimensional echocardiography of normal and pathologic mitral valve: a comparison with two-dimensional transesophageal echocardiography. *J Am Coll Cardiol.* 1996; 27:1502–10. [PubMed: 8626966]
29. Cheng TO, Xie MX, Wang XF, Li ZA, Hu G. Evaluation of mitral valve prolapse by four-dimensional echocardiography. *Am Heart J.* 1997; 133:120–9. [PubMed: 9006300]
30. Hozumi T, Yoshikawa J, Yoshida K, Akasaka T, Takagi T, Yamamuro A. Assessment of flail mitral leaflets by dynamic three-dimensional echocardiographic imaging. *Am J Cardiol.* 1997; 79:223–5. [PubMed: 9193033]
31. Chauvel C, Bogino E, Clerc P, Fernandez G, Vernhet JC, et al. Usefulness of three-dimensional echocardiography for the evaluation of mitral valve prolapse: an intraoperative study. *J Heart Valve Dis.* 2000; 9:341–9. [PubMed: 10888088]
32. Ahmed S, Nanda NC, Miller AP, Nekkanti R, Yousif AM, et al. Usefulness of transesophageal three-dimensional echocardiography in the identification of individual segment/scallop prolapse of the mitral valve. *Echocardiography.* 2003; 20:203–9. [PubMed: 12848691]
33. Clavel MA, Mantovani F, Malouf J, Michelena HI, Vatury O, et al. Dynamic phenotypes of degenerative myxomatous mitral valve disease: quantitative 3-dimensional echocardiographic study. *Circ Cardiovasc Imaging.* 2015;8.
34. Hutchins GM, Moore GW, Skoog DK. The association of floppy mitral valve with disjunction of the mitral annulus fibrosus. *N Engl J Med.* 1986; 314:535–40. [PubMed: 3945291]
35. Eriksson MJ, Bitkover CY, Omran AS, David TE, Ivanov J, et al. Mitral annular disjunction in advanced myxomatous mitral valve disease: echocardiographic detection and surgical correction. *J Am Soc Echocardiogr.* 2005; 18:1014–22. [PubMed: 16198877]
36. Carmo P, Andrade MJ, Aguiar C, Rodrigues R, Gouveia R, Silva JA. Mitral annular disjunction in myxomatous mitral valve disease: a relevant abnormality recognizable by transthoracic echocardiography. *Cardiovasc Ultrasound.* 2010; 8:53. [PubMed: 21143934]
37. Lee AP, Jin CN, Fan Y, Wong RHL, Underwood MJ, Wan S. Functional Implication of Mitral Annular Disjunction in Mitral Valve Prolapse: A Quantitative Dynamic 3D Echocardiographic Study. *JACC Cardiovasc Imaging.* 2017
38. Gelfand EV, Hughes S, Hauser TH, Yeon SB, Goepfert L, et al. Severity of mitral and aortic regurgitation as assessed by cardiovascular magnetic resonance: optimizing correlation with Doppler echocardiography. *J Cardiovasc Magn Reson.* 2006; 8:503–7. [PubMed: 16755839]
39. Han Y, Peters DC, Salton CJ, Bzymek D, Nezafat R, et al. Cardiovascular magnetic resonance characterization of mitral valve prolapse. *JACC Cardiovasc Imaging.* 2008; 1:294–303. [PubMed: 19356441]
40. Delling FN, Kang LL, Yeon SB, Kissinger KV, Goddu B, et al. CMR predictors of mitral regurgitation in mitral valve prolapse. *JACC Cardiovasc Imaging.* 2010; 3:1037–45. [PubMed: 20947049]
41. Chuang ML, Hibberd MG, Salton CJ, Beaudin RA, Riley MF, et al. Importance of imaging method over imaging modality in noninvasive determination of left ventricular volumes and ejection fraction: assessment by two- and three-dimensional echocardiography and magnetic resonance imaging. *J Am Coll Cardiol.* 2000; 35:477–84. [PubMed: 10676697]

42. Fujita N, Chazouilleres AF, Hartiala JJ, O'Sullivan M, Heidenreich P, et al. Quantification of mitral regurgitation by velocity-encoded cine nuclear magnetic resonance imaging. *J Am Coll Cardiol*. 1994; 23:951–8. [PubMed: 8106701]
43. Basso C, Perazzolo Marra M, Rizzo S, De Lazzari M, Giorgi B, et al. Arrhythmic Mitral Valve Prolapse and Sudden Cardiac Death. *Circulation*. 2015; 132:556–66. [PubMed: 26160859]
44. Perazzolo Marra M, Basso C, De Lazzari M, Rizzo S, Cipriani A, et al. Morphofunctional Abnormalities of Mitral Annulus and Arrhythmic Mitral Valve Prolapse. *Circ Cardiovasc Imaging*. 2016; 9:e005030. [PubMed: 27516479]
45. Edwards NC, Moody WE, Yuan M, Weale P, Neal D, et al. Quantification of left ventricular interstitial fibrosis in asymptomatic chronic primary degenerative mitral regurgitation. *Circ Cardiovasc Imaging*. 2014; 7:946–53. [PubMed: 25140067]
46. Bui AH, Roujol S, Foppa M, Kissinger KV, Goddu B, et al. Diffuse myocardial fibrosis in patients with mitral valve prolapse and ventricular arrhythmia. *Heart*. 2017; 103:204–9. [PubMed: 27515954]
47. Ghosh N, Al-Shehri H, Chan K, Mesana T, Chan V, et al. Characterization of mitral valve prolapse with cardiac computed tomography: comparison to echocardiographic and intraoperative findings. *Int J Cardiovasc Imaging*. 2012; 28:855–63. [PubMed: 21604082]
48. Hancock EW, Cohn K. The syndrome associated with midsystolic click and late systolic murmur. *Am J Med*. 1966; 41:183–96. [PubMed: 4161768]
49. Strahan NV, Murphy EA, Fortuin NJ, Come PC, Humphries JO. Inheritance of the mitral valve prolapse syndrome. Discussion of a three-dimensional penetrance model. *Am J Med*. 1983; 74:967–72. [PubMed: 6859065]
50. Weiss AN, Mimbs JW, Ludbrook PA, Sobel BE. Echocardiographic detection of mitral valve prolapse. Exclusion of false positive diagnosis and determination of inheritance. *Circulation*. 1975; 52:1091–6. [PubMed: 1182954]
51. Delling FN, Rong J, Larson MG, Lehman B, Osypiuk E, et al. Familial clustering of mitral valve prolapse in the community. *Circulation*. 2015; 131:263–8. [PubMed: 25361552]
52. Disse S, Abergel E, Berrebi A, Houot AM, Le Heuzey JY, et al. Mapping of a first locus for autosomal dominant myxomatous mitral-valve prolapse to chromosome 16p11.2–p12.1. *Am J Hum Genet*. 1999; 65:1242–51. [PubMed: 10521289]
53. Freed LA, Acierno JS Jr, Dai D, Leyne M, Marshall JE, et al. A locus for autosomal dominant mitral valve prolapse on chromosome 11p15.4. *Am J Hum Genet*. 2003; 72:1551–9. [PubMed: 12707861]
54. Nesta F, Leyne M, Yosefy C, Simpson C, Dai D, et al. New locus for autosomal dominant mitral valve prolapse on chromosome 13: clinical insights from genetic studies. *Circulation*. 2005; 112:2022–30. [PubMed: 16172273]
55. Kyndt F, Schott JJ, Trochu JN, Baranger F, Herbert O, et al. Mapping of X-linked myxomatous valvular dystrophy to chromosome Xq28. *Am J Hum Genet*. 1998; 62:627–32. [PubMed: 9497244]
56. Kyndt F, Gueffet JP, Probst V, Jaafar P, Legendre A, et al. Mutations in the gene encoding filamin A as a cause for familial cardiac valvular dystrophy. *Circulation*. 2007; 115:40–9. [PubMed: 17190868]
57. Nakamura F, Stossel TP, Hartwig JH. The filamins: organizers of cell structure and function. *Cell Adh Migr*. 2011; 5:160–9. [PubMed: 21169733]
58. Sasaki A, Masuda Y, Ohta Y, Ikeda K, Watanabe K. Filamin associates with Smads and regulates transforming growth factor-beta signaling. *J Biol Chem*. 2001; 276:17871–7. [PubMed: 11278410]
59. Sauls K, de Vlaming A, Harris BS, Williams K, Wessels A, et al. Developmental basis for filamin-A-associated myxomatous mitral valve disease. *Cardiovasc Res*. 2012; 96:109–19. [PubMed: 22843703]
60. Durst R, Sauls K, Peal DS, deVlaming A, Toomer K, et al. Mutations in DCHS1 cause mitral valve prolapse. *Nature*. 2015; 525:109–13. [PubMed: 26258302]
61. Dina C, Bouatia-Naji N, Tucker N, Delling FN, Toomer K, et al. Genetic association analyses highlight biological pathways underlying mitral valve prolapse. *Nat Genet*. 2015; 47:1206–11. [PubMed: 26301497]

62. Bowers D. Pathogenesis of primary abnormalities of the mitral valve in Marfan's syndrome. *Br Heart J.* 1969; 31:679–83. [PubMed: 5358147]
63. Dietz HC, Cutting GR, Pyeritz RE, Maslen CL, Sakai LY, et al. Marfan syndrome caused by a recurrent de novo missense mutation in the fibrillin gene. *Nature.* 1991; 352:337–9. [PubMed: 1852208]
64. Mizuguchi T, Collod-Beroud G, Akiyama T, Abifadel M, Harada N, et al. Heterozygous TGFBR2 mutations in Marfan syndrome. *Nat Genet.* 2004; 36:855–60. [PubMed: 15235604]
65. Ng CM, Cheng A, Myers LA, Martinez-Murillo F, Jie C, et al. TGF-beta-dependent pathogenesis of mitral valve prolapse in a mouse model of Marfan syndrome. *J Clin Invest.* 2004; 114:1586–92. [PubMed: 15546004]
66. Habashi JP, Judge DP, Holm TM, Cohn RD, Loeys BL, et al. Losartan, an AT1 antagonist, prevents aortic aneurysm in a mouse model of Marfan syndrome. *Science.* 2006; 312:117–21. [PubMed: 16601194]
67. Delling FN, Gona P, Larson MG, Lehman B, Manning WJ, et al. Mild expression of mitral valve prolapse in the Framingham offspring: expanding the phenotypic spectrum. *J Am Soc Echocardiogr.* 2014; 27:17–23. [PubMed: 24206636]
68. Avierinos JF, Detaint D, Messika-Zeitoun D, Mohty D, Enriquez-Sarano M. Risk, determinants, and outcome implications of progression of mitral regurgitation after diagnosis of mitral valve prolapse in a single community. *Am J Cardiol.* 2008; 101:662–7. [PubMed: 18308017]
69. Enriquez-Sarano M, Avierinos JF, Messika-Zeitoun D, Detaint D, Capps M, et al. Quantitative determinants of the outcome of asymptomatic mitral regurgitation. *N Engl J Med.* 2005; 352:875–83. [PubMed: 15745978]
70. Enriquez-Sarano M, Basmadjian AJ, Rossi A, Bailey KR, Seward JB, Tajik AJ. Progression of mitral regurgitation: a prospective Doppler echocardiographic study. *J Am Coll Cardiol.* 1999; 34:1137–44. [PubMed: 10520803]
71. Avierinos JF, Brown RD, Foley DA, Nkomo V, Petty GW, et al. Cerebral ischemic events after diagnosis of mitral valve prolapse - A community-based study of incidence and predictive factors. *Stroke.* 2003; 34:1339–44. [PubMed: 12738894]
72. Nishimura RA, McGoon MD, Shub C, Miller FA Jr, Ilstrup DM, Tajik AJ. Echocardiographically documented mitral-valve prolapse. Long-term follow-up of 237 patients. *N Engl J Med.* 1985; 313:1305–9. [PubMed: 4058522]
73. Enriquez-Sarano M, Seward JB, Bailey KR, Tajik AJ. Effective regurgitant orifice area: a noninvasive Doppler development of an old hemodynamic concept. *J Am Coll Cardiol.* 1994; 23:443–51. [PubMed: 8294699]
74. Sriram CS, Syed FF, Ferguson ME, Johnson JN, Enriquez-Sarano M, et al. Malignant bileaflet mitral valve prolapse syndrome in patients with otherwise idiopathic out-of-hospital cardiac arrest. *J Am Coll Cardiol.* 2013; 62:222–30. [PubMed: 23563135]

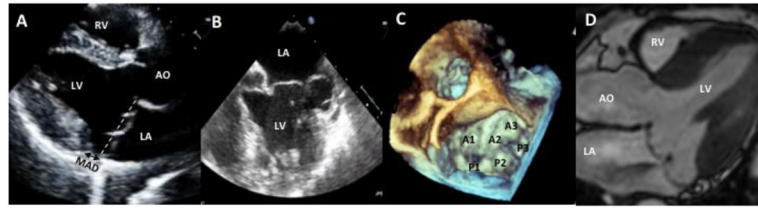


Figure 1.

Example of bileaflet mitral valve prolapse (A–D). Prolapse of the anterior and posterior mitral valve leaflets demonstrated in (A) a long-axis view of a 2-dimensional (2D) transthoracic echocardiogram (leaflets are displaced more than 2 mm beyond the annulus, shown as a dotted line), (B) a mid-esophageal 4-chamber view of a 2D transesophageal (TEE) echocardiogram, (C) a 3-dimensional (3D) TEE *en face* or surgical view (A1, A2, A3 and P1, P2, P3 are the lateral, middle, and medial anterior and posterior scallops, respectively), and (D) a cardiac magnetic resonance (CMR) steady state free processing (SSFP) long-axis view. AO = aorta; LA = left atrium; LV = left ventricle; RV = right ventricle; MAD = mitral-annular disjunction (separation between the left atrial wall at the level of mitral valve junction and the LV free wall).

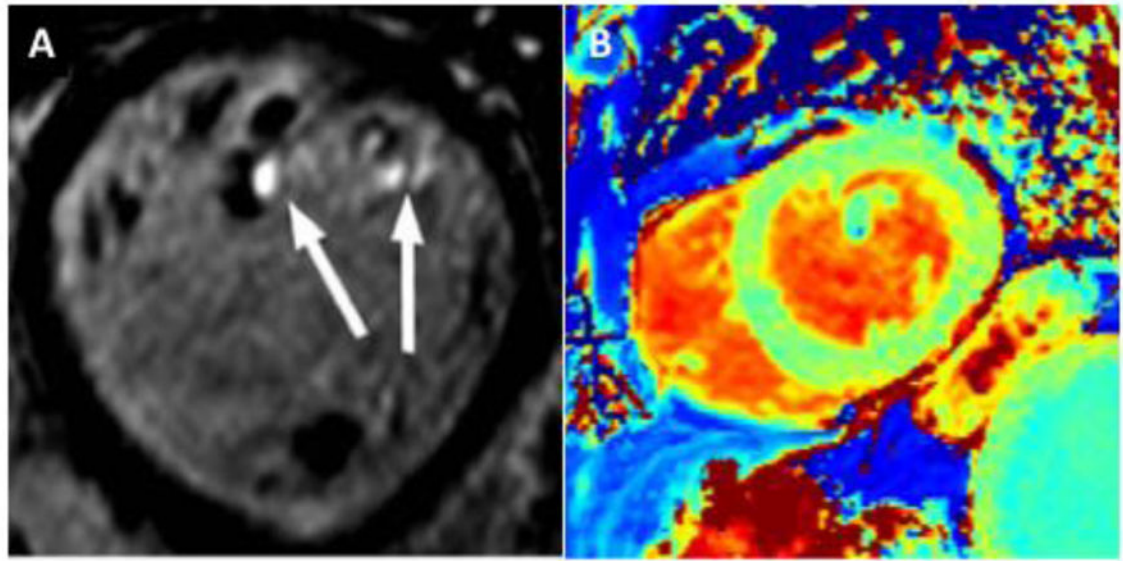


Figure 2. Examples of focal and diffuse myocardial fibrosis in mitral valve prolapse (MVP). Short-axis view with three-dimensional late-gadolinium enhancement showing fibrosis of the papillary muscle tips (arrows) in a patient with bileaflet MVP and mild mitral regurgitation (A); precontrast T1 map with increased native T1 (1145 ms) indicating interstitial myocardial fibrosis in a different MVP patient with moderate-severe mitral regurgitation (B).

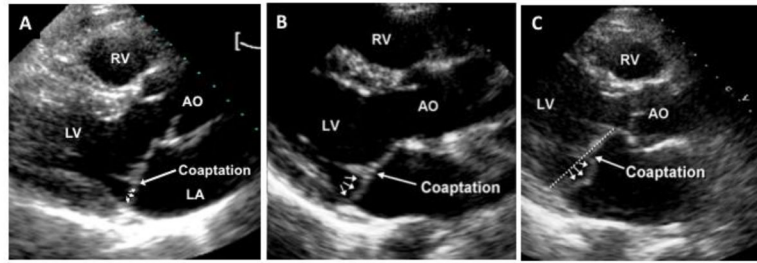


Figure 3.

Phenotypic spectrum of mitral valve prolapse (MVP). 2-dimensional echocardiographic parasternal long-axis images demonstrating (A) minimal systolic displacement, (B) anterior abnormal coaptation, and (C) posterior MVP. All show posterior leaflet bulging (arrows) relative to the anterior leaflet, but only MVP shows diagnostic superior leaflet displacement relative to the mitral annulus (dotted line) into the left atrium (LA). Posterior MVP and abnormal anterior coaptation are similar with regards to an increased coaptation height and an elongated posterior leaflet. Minimal systolic displacement shows posteriorly coapting leaflets, as seen in normal patients. AO = aorta; LV = left ventricle; RV = right ventricle.